Development of a Robust Computational Design Simulator for Industrial Deformation Processes

by

Zabaras, Nicholas
Materials Process Design and Control Laboratory
Sibley School of Mechanical and Aerospace Engineering
188 Frank H. T. Rhodes Hall
Cornell University, Ithaca, NY 14853-3801
Email: zabaras@cornell.edu

ABSTRACT

As part of this continuing DMII-funded NSF project, computationally rigorous gradient-based optimization methodologies are being addressed for a virtual materials process design that is based on quantified product quality and accounts for process targets and constraints including economic aspects. Computational design techniques will be developed that can be used to select the necessary sequence of forming and intermediate thermal-stage processes, select appropriate dies and preforms and control/design the various process parameters such that, for a given raw material with a given initial geometry, one can obtain a final product with desired microstructure and shape under various process constraints and with minimal utilization rates and overall cost.

A framework for preform as well as process parameter optimization for single- and multi-stage metal forming processes is considered. The design of each individual process will be performed using gradient-optimization techniques that are based on a rigorous continuum sensitivity analysis. Multi-stage sensitivity algorithms are proposed that allow the sensitivity fields of individual processes to be used in multi-stage process design. Optimal microstructure evolution paths, ideal forming techniques and knowledge based expert systems will be used to select the required sequence of processes and to develop feasible initial designs. The reliability of the design process will be quantified with respect to uncertainties in the physical and mathematical model. The combination of ideal forming and sensitivity analysis provides a powerful virtual design environment for deformation processes.

To focus the proposed work towards the design of industrial deformation processes, we will emphasize the use of polycrystalline constitutive models that account for the induced microstructure changes during processing, realistic modeling and representation of frictional and contact conditions, complicated die and preform geometries and practical process constraints and objectives. Materials and aerospace manufacturing industries will also collaborate with us during this investigation thus allowing industrial use of the proposed techniques and providing the Cornell team with valuable technical information.

The use of ideal forming to obtain an initial design and a continuum sensitivity analysis for computing the optimal process design constitutes a mathematically and physically rigorous and computationally effective methodology for process design of metallic components in advanced manufacturing applications. These developments will lead to a virtual process laboratory that will assist industry in reducing lead time for process and product development, in trimming the cost of an extensive experimental trial-and-error process development effort, in developing processes for tailored material properties and in increasing volume/time yield.

1 INTRODUCTION: OBJECTIVES AND INDUSTRIAL SIGNIFICANCE

The use of computer technology for simulation of metal deformation processes has increased dramatically over the last 30 years. The detailed simulation of the metal flow during plastic deformation using the finite element method is now common place and reliable. In spite of this increased use of simulation technology, selection of actual process design variables (number of different dies, shapes of dies and preforms, etc.)

still requires a significant amount of expert knowledge that can be obtained only through experience. To overcome this dependency on a small group of industry experts and to reach designs that are more robust and ultimately less costly, reliable optimization-based design techniques for plastic deformation need to be developed, that parallel the developments that have proven successful in the area of structural design.

The complexity of metal forming design is apparent considering the coupled non-linear physical mechanisms that need to be accounted for such as (a) large deformation plasticity, (b) deformation induced microstructure evolution, (c) time varying contact and friction conditions, (d) thermal effects and mechanical dissipation and (e) damage accumulation leading to material rupture. The role of these mechanisms in the processing of the initial workpiece to yield the final product is paramount. Metal forming process design therefore requires the accurate description and control of these deformation mechanisms in order to achieve design objectives that may consist of the simultaneous satisfaction of one or more of the competing criteria defined in Box 1.

- Desired shape of the final product
- Minimization of material usage
- Uniform deformation in the final product
- Minimum required work or forming force
- Desired microstructure in the final product
- Desired residual stress distribution
- Minimum deformation and wear of the die
- Required level of porosity in the final product

Box 1: Typical objectives in hot forming design.

The design process is often subject to various processing constraints (Box 2). The design objectives of Box 1 can be achieved by one or more of the design mechanisms of Box 3.

- maximum available press load capacity and press speeds
- window of processing temperatures
- final product quality (e.g. control of the peripheral coarse grain (PCG) structure in extrusion processes)
- material utilization and cost
- processing temperature
- maximum allowable strain rates

Box 2. Typical process design constraints.

In industrial forming applications, the objectives indicated in Box 1 are seldom simple enough to be achieved in a single forming operation. As a result, intermediate deformation or preforming steps are used to efficiently transform the initial geometry into a final shape with desired material properties.

- Identification and selection of intermediate stages
- Appropriate design of the forming die surfaces
- Design of the geometry of the initial and intermediate billets (preform design)
- Design of the material state (microstructure) of the initial billet
- Appropriate selection of the process parameters (ram speed, lubrication conditions, operating temperature, etc.)

Box 3. Design variables in hot forming design.

A forming sequence can be viewed at two levels for the purpose of design (a) the broad identification of the number, type and order of forming and heat-treatment operations that make up the sequence (e.g. forward extrusion, open die forging) and (b) the specific identification and selection of design variables in each of the forming operations (e.g. ram speed in extrusion, die shape or stroke in a preforming stage).

There are many factors that result in poor material utilization rates, high cost of process equipment and lack of complete control on final product quality, in fact, so many that it is impossible for a non-expert designer to simultaneously consider all of them while making decisions. In this work, we propose to develop computational design algorithms that can effectively address multi-stage design problems, a representative example of which is shown in Fig. 1 and defined as follows:

> *Determine initial billet dimensions, preform, blocker, and finisher die geometries, workpiece temperatures, press speeds, and intermediate heat treatment parameters, to minimize overall cost while meeting sonic inspection geometry requirements, achieve control of microstructure distribution and die fill, avoid geometric defects and residual stresses and ensure that all this is done using existing equipment.*

It is the objective of this continuing NSF project to develop a mathematically and computationally rigorous gradient-based optimization methodology for a virtual materials process design that is based on quantified product quality and accounts for process targets and constraints including economic aspects. The virtual design simulator depicted in Box 4 includes the development of an innovative sensitivity analysis consistent to a virtual direct process simulator. This sensitivity analysis should be capable to provide the sensitivity fields of deformation and material state with respect to the design parameters under consideration.

- 1. Mathematical representation of the design objective
- 2. Selection of the sequence of processes (stages) and initial process parameter designs using knowledge based expert systems, microstructure evolution paths and/or ideal forming techniques
- 3. Selection of the design variables (e.g. die and preform parametrization)
- 4. Selection of a virtual direct process model
- 5. Interactive optimization environment
- 6. Continuum multi-stage process sensitivity analysis consistent with the direct process model
- 7. Optimization algorithms
- 8. Assessment of automatic process optimization
- 9. Reliability of the optimal design to physical and computational model errors

Box 4: A computational design simulator for forming processes.

A framework for preform as well as process parameter optimization is discussed here for single- and multi-stage metal forming processes. The design of each individual process is performed using gradient-optimization techniques that are based on a rigorous continuum sensitivity analysis. Multi-stage sensitivity algorithms are also being developed that allow the sensitivity fields of individual processes to be used in multi-stage process design. Optimal microstructure evolution paths, ideal forming techniques and knowledge based expert systems will be used to select the required sequence of processes and to develop feasible initial designs. The combination of ideal forming and sensitivity analysis provides a powerful virtual design environment for deformation processes (Box 4).

Successful implementation of the various proposed developments will lead to a virtual process laboratory that will assist industry in reducing lead time for process development, in trimming the cost of an extensive experimental trial-and-error process development effort, in developing processes for tailored material properties and in increasing volume/time yield.

2 LITERATURE REVIEW

A systematic study of preform and die design problems is given in [1]–[7]. In the work of Kobayashi and others [1]–[4], the simulation process proceeds starting from the final desired shape. Such reverse material flow is a fictitious construct and cannot lead to physically and mathematically realistic designs. A popular preform design methodology for sheet metal forming processes is the ideal forming theory which assumes that material elements deform along minimum plastic work paths. Ideal forming processes can be used to obtain a final product shape with uniform strain distribution and yield as solutions initial and intermediate configurations of the workpiece [8]-[9]. Ideal forming methods assume frictionless contact conditions. Extension to bulk forming processes may allow the use of ideal forming solutions as initial designs to more elaborate algorithms and such ideas will be further explored in our work.

Applications of knowledge based systems, neural networks and genetic algorithms for design of material processes are given in [10]-[16]. Once trained using simulation runs of the process, the neural network can be used for design. Neural networks are useful, when one is concerned with the design of a single process where different objectives may be required by the process engineer at various times. However if the network has to deal with the design of different processes, then the method loses its merit. Genetic algorithms are based on the survival of the fittest design in a population of designs. The design variable is represented as a binary string and the optimal design is achieved after generations of population are obtained by operations of reproduction, cross-over and mutation. Genetic algorithms are powerful techniques which can handle discrete design data with ease (e.g. number of stages in multi-stage design). The above methods are very inefficient compared to gradient based methods for the case of continuous design data and for systems where the evaluation of the objective function and constraints is costly.

The response surface method (RSM) has been adopted to approximate some highly complex system responses [17]. This method appears effective when the precise description of a true mathematical or gradient relation is impossible or difficult, for example is has been used in sheet forming to describe the sheet thickness distribution in terms of the die shape or process parameters [18]. As a global approximation method, RSM may avoid being trapped in a local minimum, and thus can serve for a pre-optimization search. However, RSM requires solution of a large number of direct problems and with an increased number of design variables it results in a computational cost that is prohibitively high [17].

Using sensitivity analysis to address deformation design and identification problems is recently receiving extensive attention [19]-[21]. Sensitivities can be computed either by employing finite differences (FDM), direct differentiation (DDM) or the adjoint variable method. The adjoint method has been quite popular for design and control problems in fluid mechanics/heat transfer [22] and some applications to deformation problems have been reported as well [23]–[24]. The adjoint method is a particularly tractable technique for systems with continuous design variables [22] and a single design objective. In the DDM method, one solves for the response sensitivities simultaneously with the solution of the direct deformation problem. On the other hand, the FDM involves an additional solution of the direct deformation problem for a perturbed set of shape parameters. In addition to significant computer resources required for solving the direct problem multiple times, difficulties arise in such calculations for complex forming processes where the computed FDM sensitivity fields are corrupted by the numerical error in the solution of the direct analysis.

The acronym DDM is used in the literature to refer to a wide spectrum of algorithms regardless of the level at which the design differentiation is performed. In our earlier work, the equations governing the sensitivity fields were computed at the continuum level (from now on to be referred to as the *continuum sensitivity method*, CSM) [25], [26]. In an alternate discrete sensitivity description, the sensitivity equations are derived by design differentiation of their discrete counterparts in the direct problem [27]–[29]. The final scheme refers to the differentiation of the direct deformation simulator at the level of the numerical code [30]. Such automatic differentiation techniques provide a powerful tool that however fails to exploit the linear nature of the sensitivity problem. The CSM method is chosen in our work as the preferred method for evaluating sensitivities in deformation processing.

Most of the developments in the sensitivity analysis of metal forming processes use the flow formulation and are limited to steady state applications [31]-[33]. The sensitivity analysis of non-steady state deformations using the solid formulation and small deformation elasto-plasticity theory can be found in [34]–[35]. Sensitivity analysis in the finite deformation regime for the purpose of parameter identification has been carried out in [36]. A number of challenges remain in the accurate and effective computation of sensitivity fields for practical engineering problems that involve frictional contact. A scheme to evaluate the response sensitivities involving the Coulomb frictional contact of thin shell structures is presented in [37]. A sensitivity analysis for frictional metal forming processes in steady state using a flow formulation is presented in [38]. More recently, a sensitivity analysis of a non-steady state open-die forging process has been carried out in [39]. However, the results reported in [39] are not accurate indicating difficulties with the proposed formulation. Additional work on optimization of metal forming processes using a gradient based approach and a flow FEM formulation is given in [40]-[45]. The limited number of publications in multi-stage forming process design include [46], [47].

In addition to achieving a high dimensional precision of geometrical shape, an important design objective is based on the optimal control of microstructure evolution [48]. In spite of its imperative practical significance, there have been far few reports even for single stage forming processes [49]–[51].

This is partially due to the difficulties in identifying a relation between the required design variables and the microstructure development mechanisms such as dynamic/static recovery, recrystallization and grain growth. In the existing studies, moreover, it is found that the limits of a single stage process to the selection of design variables and feasible space make the improvement of optimized microstructure insignificant [49], [50], thus further emphasizing the need for multi-stage process design. In recent years, the simulations of the microstructure evolution and thermo-mechanical mechanisms have received extensive attention for a wide range of metals. Empirical formulations useful for process design have been developed in [52], [53] and can be used to identify the relation between the microstructure and thermo-mechanical response fields.

2.1 BACKGROUND WORK

A review of the direct deformation process simulator utilized in our design developments can be found in [54]. In the remaining of this report, a multiplicative framework of the form $\boldsymbol{F} = \boldsymbol{F}^e \bar{\boldsymbol{F}}^p \boldsymbol{F}^\theta$ [55] is assumed with state variable based inelastic models such as those given in [56]-[58].

The most distinct element of our analysis is the development of a unique continuum framework for sensitivity analysis of large deformations. As a demonstration of ideas we concentrate on preform design and provide here a precise definition of the shape derivatives of Lagrangian and Eulerian fields with respect to the preform shape $\partial \boldsymbol{B}_0$ in a given forming process (Fig. 2). The key element of this definition is that the configuration $\boldsymbol{B}_0$ (at $t = t_0$) with respect to which all Lagrangian fields are expressed is not fixed in a preform design process. To allow shape differentiation with respect to the preform shape, a reference configuration $\boldsymbol{B}_R$ with $\boldsymbol{Y} \in \boldsymbol{B}_R$ is defined so that the configuration $\boldsymbol{B}_0$ is completely described by a smooth geometric reference map of the form $\boldsymbol{x}_0 = \hat{\boldsymbol{x}}_0 (\boldsymbol{Y}; \boldsymbol{\beta})$, where in general $\boldsymbol{\beta}$ are smooth functions that define the whole or parts of $\partial \boldsymbol{B}_0$. The spatial configuration $\boldsymbol{B}_t$ at time t with $\boldsymbol{x} = \hat{\boldsymbol{x}} (\boldsymbol{x}_0, t) \in \boldsymbol{B}_t$ is given by the motion of the body as $\boldsymbol{x} = \hat{\boldsymbol{x}} (\hat{\boldsymbol{x}}_0 (\boldsymbol{Y}; \boldsymbol{\beta}), t) = \tilde{\boldsymbol{x}} (\boldsymbol{Y}, t; \boldsymbol{\beta})$.

The shape derivative, $\overset{\circ}{\boldsymbol{\Phi}} (\boldsymbol{Y}, t; \boldsymbol{\beta})$ of a tensor valued function $\boldsymbol{\Phi}$ is the total Gateaux derivative of $\boldsymbol{\Phi}$ in the direction of $\Delta \boldsymbol{\beta}$ computed at $\boldsymbol{\beta}$. Comparison of the fields $\boldsymbol{\Phi}(\boldsymbol{\beta})$ and $\boldsymbol{\Phi}(\boldsymbol{\beta} + \Delta \boldsymbol{\beta})$ is here made at points of the reference (fixed) configuration $\boldsymbol{B}_R$ (see Fig. 2 for the definition of $\overset{\circ}{\boldsymbol{F}}$) [59], [60].

A continuum sensitivity large deformation problem has been defined for the calculation of the sensitivities of the deformation gradient, material state and plastic deformation with respect to die surfaces and preforms. Figure 3 presents the main structure of the continuum sensitivity problem [59]–[63], where three incremental sensitivity subproblems have been defined by taking the derivative of the corresponding continuum subproblems of the direct analysis with respect to the preform shape. The weak form of the shape derivative of the equilibrium equation can be shown to take the following form [63]:

$$\int_{\boldsymbol{B}_o} \overset{\circ}{\boldsymbol{P}} \bullet \nabla_X \tilde{\boldsymbol{\eta}} dV_o - \int_{\boldsymbol{B}_o} \left(\boldsymbol{P} \left[\nabla_X \bullet \boldsymbol{L}_{\boldsymbol{\beta}}{}^T \right] \right) \bullet \tilde{\boldsymbol{\eta}} dV_o - \int_{\boldsymbol{B}_o} \left(\boldsymbol{P} \boldsymbol{L}_{\boldsymbol{\beta}}{}^T \right) \bullet \nabla_X \tilde{\boldsymbol{\eta}} \, dV_o = \int_{\boldsymbol{\Gamma}} \left\{ \overset{\circ}{\boldsymbol{\lambda}} - \left[\boldsymbol{L}_{\boldsymbol{\beta}} \bullet (\boldsymbol{N} \otimes \boldsymbol{N}) \right] \boldsymbol{\lambda} \right\} \bullet \tilde{\boldsymbol{\eta}} \, dA_o \tag{1}$$

where $\boldsymbol{P}$ is the Piola I stress, the design velocity gradient $\boldsymbol{L}_{\boldsymbol{\beta}}$ is given as $\boldsymbol{L}_{\boldsymbol{\beta}} = \overset{\circ}{\boldsymbol{F}}_R \ \boldsymbol{F}_R^{-1}$, and the reference deformation gradient $\boldsymbol{F}_R$ (see Fig. 2) is given as $\boldsymbol{F}_R(\boldsymbol{Y}; \boldsymbol{\beta}) = \nabla_Y \boldsymbol{X}$.

The equation above defines the kinematic sensitivity problem that (in a preform design problem) can be used to find the sensitivity of the deformation with respect to the preform shape (Fig. 3). In addition to the linear coupling of this problem with the sensitivity constitutive problem, the contact sensitivity problem must be solved. As a result of the non-smooth nature of the contact/friction conditions, the calculation of the sensitivity of contact traction components is a non-trivial task that has received minor attention even though contact and friction are the driving mechanisms in many forming design problems. Non-smooth contact/frictional behavior results from the abrupt variation of the normal traction component at impending contact and from the abrupt variation of tangential traction component at the stick-slip transition. To allow for the differentiability of the direct contact/frictional conditions *regularizing assumptions* were introduced that constrain *transition from stick to slip and/or from contact to non-contact (or vice-versa) not to occur at a material point as a result of a perturbation to the design parameters*. Detailed discussion on this form of regularization can be found in [62], [63].

Design problems such as those in Box 1 take the form of minimizing a proper cost functional. For the case of a single objective with multiple constraints, we can write the following optimization problem:[1] $\min_{\boldsymbol{\beta}}\ f(\boldsymbol{\beta}),\ g_i(\boldsymbol{\beta}) \leq 0,\ h_j(\boldsymbol{\beta}) = 0$. In gradient based optimization techniques [64], the gradient of the objective function and constraints with respect to the design variables is needed. Let us consider N scalar design parameters β_i and the corresponding basis functions ϕ_i which represent the design space $\boldsymbol{\beta}$. Let us assume that f depends on $\boldsymbol{\beta}$ through a deformation related Lagrangian field Z. The gradient $\nabla \boldsymbol{Z}$ is defined in the above parameter space using the solution of N continuum sensitivity problems.

3 PROPOSED WORK AND RESEARCH PLAN

The development of a framework for the design of multi-stage forming processes will be discussed here including algorithms for the selection of the sequence of processes and for the design of individual processes. Initial design sequences will be defined based on ideal forming methods, whereas the optimal design of the individual processes will be performed by a mathematically and physically rigorous continuum sensitivity analysis for multi-stage forming derived using the framework shown in Fig. 3 for single-stage processes. These developments are implemented using an object-oriented approach that allows a unified handling of various processes, material models, design criteria, design variables and process constraints.

3.1 Need for and Essential Requirements of a Robust Industrial Forming Design Simulator

Even though, there are some robust and accurate direct forming simulators, there are no industrial forming design simulators available as of today. There is indeed a significant need to develop a design simulator capable of handling complex industrial forming design problems for technologically advanced applications such as in aerospace manufacturing. As part of this NSF sponsored project and with additional support from the U.S. Air Force and industry, we have initiated an intensive effort to resolve all technical issues towards the development of such a design simulator. Box 5 briefly highlights the basic features that we propose to develop and include in this design simulator.

3.2 A Framework for Multi-Stage Process Design

In most industrial forming applications, the desired objectives indicated in Box 1 are seldom simple enough to be achieved in a single forming operation. As a result, intermediate deformation or preforming steps are used to efficiently transform the initial geometry into a final shape with desired material properties. Thermal processing is also used in between deformation stages to control the microstructure. Optimization of multi-stage processes may be viewed as the design of the forming sequence that converts the initial workpiece to the final product while meeting desired manufacturing objectives and satisfying process constraints. The directed graph of Fig. 4 is an abstract representation of possible process sequences typical of multi-stage design. Each *node* in the graph corresponds to a preform and represents the beginning and/or end of a new processing stage (Thermal/Deformation/Thermomechanical). The preform is characterized by the shape as well as its mechanical and thermal state.

In the present work, the identification of the forming operations will be performed using knowledge based systems, ideal forming techniques and optimal microstructure evolution paths. The design decisions for the individual selected processes will be performed using a gradient optimization scheme based on an innovative continuum sensitivity analysis appropriate for multi-stage deformation processes. Such a procedure will permit with ease the analysis of multi-stage processes with a large number of stages. Knowledge based expert systems rely on the mathematical abstract representation of the manufacturing process, the representation of a-priori knowledge about various processes in the form of simple (if-then-else) rules and a powerful reasoning system (inference engine) [13], [65]. The representation of the process in Fig. 4 as a directed graph is for this purpose.

[1]For example, the design problem of obtaining a uniform material state s in the final product $\boldsymbol{B}_f$ can be written as follows: $\min_{\boldsymbol{\beta}} \int_{\boldsymbol{B}_f} [\ s(\boldsymbol{x},\boldsymbol{\beta}) \ - \ \bar{s}(\boldsymbol{x},\boldsymbol{\beta})\ ]^2\ dV$, where $\bar{s}(\boldsymbol{x},\boldsymbol{\beta}) = \dfrac{\int_{\boldsymbol{B}_f} s(\boldsymbol{x},\boldsymbol{\beta})\ dV}{\int_{\boldsymbol{B}_f} dV}$ and $\boldsymbol{\beta}$ are appropriate design parameters.

- (1) The design simulator needs to be efficient and thus methodologies that require extensive direct forming simulations (e.g. surface response methodologies, etc.) are not acceptable.
- (2) The simulator should be oriented towards the design of multi-stage forming processes and coupling of consistent multi-dimensional direct & sensitivity analyses with knowledge-based, ideal forming & microstructure evolution algorithms for stage selection is essential.
- (3) Remeshing & data transfer techniques currently applicable in the direct analysis should be extended to the sensitivity analysis to allow handling of complex deformations.
- (4) A mathematically rigorous handling of the sensitivity of the contact/frictional conditions needs to be provided since it is such conditions that drive most forming design problems. Abrupt contact, fold-over and non-smooth deformable dies need to be accounted for.
- (5) Incompressibility and element locking issues under plastic deformations should be extended to the sensitivity analyses. One should allow for various type of finite elements that are acceptable in both the direct and sensitivity large plastic deformation calculations. For example, enhanced strain like methods need to be extended to sensitivity analysis in order to preserve consistency of the sensitivity data with the direct fields.
- (6) The direct and sensitivity-design simulators should be able to account for the complex behavior of polycrystalline material models.
- (7) The design simulator should allow for the design of multiple intermediate thermal stages. In addition, the design simulator should allow the evaluation of the sensitivities of residual stresses with respect to any design variable. This unique feature is important as the process of going from one forming stage to another requires accurate evaluation of the sensitivities of residual stresses induced by the earlier forming stages.
- (8) Provide mathematically rigorous definition of mesh-independent sensitivity fields that address non-differentiability issues, shape differentiation etc. In particular, designing with respect to various variables needs to be treated with care, e.g. attention needs to be given in the interpretation of the sensitivities of any field value with respect to the die surface or the preform shape. False interpretation of such sensitivities has led to a number of published work with erroneous mathematically and physically computations.
- (9) Provide for the design of hot forming processes and for example allow for the design of the heat flux (or temperature) distribution in the die surface during the process.
- (10) Interface with commercial solid modelers and optimization tools.

Box 5: Essential features of a design simulator for industrial forming processes that we plan to address in this work.

In defining an initial feasible sequence of processes, one should take advantage of any shop-floor expertise as well as any knowledge that has been gained from the numerical simulation of various direct processes. Ideal forming or microstructure evolution paths will point to intermediate deformation paths, but it is up to the designer to interpret the ideal forming solution to a design space and that can be done in mathematical manner or using well organized a-priori information. Once an initial design has been selected, the overall design problem will be stated as an optimization problem and gradient based optimization techniques will be used to compute its solution. The importance of a good initial design in the optimization process needs to be emphasized as it will require less number of optimization iterations and in addition it may lead to a local minimum that corresponds to desired microstructural features in the final product (when using optimal microstructure evolution paths) or to minimal work (when using ideal forming techniques).

We plan to take advantage of the shop-floor expertise that will be provided by our industrial partners. In addition the numerical simulations will also provide information about the processes and there will be a significant growth in the amount of knowledge available as the design simulator is put to use. We emphasize that this knowledge-based procedure will be used only to identify feasible (possibly good) sequences and the optimization will be performed using gradient based techniques as discussed next.

3.2.1 Sensitivity analysis for the design of multi-stage forming processes

Most forged components require more than one processing operation due to the violation of one or more of process constraints. A framework is presented here to expand the shape and parameter sensitivity analyses developed for a single stage forming operation to a multi-stage process design where the broad identification (and number) of the intermediate forming operations is assumed to be a priori known. Sensitivity analysis of a multi-stage process necessarily involves the computation of both shape as well as parameter sensitivities. Unlike a single stage shape sensitivity analysis where the initial workpiece shape depends explicitly on shape design variables, the intermediate preform shape in a generic forming stage of a multi-stage process depends implicitly on the design variables (non-shape parameters) that define the processing history of the intermediate preform.

Here we introduce notions of the sensitivity of various physical fields with respect to small changes in the design variables of the forming sequence depicted in Figure 5(a). The deformation history leading to the intermediate preform which defines $\boldsymbol{B}_o$ is described as follows:

$$\boldsymbol{X} \;=\; \bar{\boldsymbol{X}}(\boldsymbol{Y}, t_o; \boldsymbol{\beta}_Y), \;\forall\; \boldsymbol{Y} \in \boldsymbol{B}_i \tag{2}$$

where $\boldsymbol{\beta}_Y$ represents the collection of design variables in all previous forming stages. The deformation in a generic (current) forming stage can be then represented as:

$$\boldsymbol{x} \;=\; \tilde{\boldsymbol{x}}(\boldsymbol{X}, t; \boldsymbol{\beta}), \;\forall\; \boldsymbol{X} \in \boldsymbol{B}_o, \; t \in [t_o, t_f] \tag{3}$$

where $\boldsymbol{\beta} = \boldsymbol{\beta}_X \cup \boldsymbol{\beta}_Y$ and $\boldsymbol{\beta}_X$ represents the (non-shape) design variables in the current forming stage. The dependence of fields $\Phi = \tilde{\Phi}(\boldsymbol{X}, t)$ on $\boldsymbol{\beta}$ can be expressed as follows:

$$\Phi = \tilde{\Phi}(\bar{\boldsymbol{X}}(\boldsymbol{Y}, t_o; \boldsymbol{\beta}_Y), t; \boldsymbol{\beta}) = \bar{\Phi}(\boldsymbol{Y}, t; \boldsymbol{\beta}) \tag{4}$$

The design differential $\overset{\circ}{\Phi}$ is defined as the total Gateaux differential of $\Phi = \bar{\Phi}(\boldsymbol{Y}, t; \boldsymbol{\beta})$, i.e.

$$\overset{\circ}{\Phi} = \left. \frac{d}{d\lambda}\, \bar{\Phi}(\boldsymbol{Y}, t; \boldsymbol{\beta} + \lambda \Delta\boldsymbol{\beta}) \right|_{\lambda=0} \tag{5}$$

In the above Equ. $\boldsymbol{\beta}$ could represent either $\boldsymbol{\beta}_X$ or $\boldsymbol{\beta}_Y$. When $\boldsymbol{\beta}$ represents the non-shape design parameters of the current forming stage i.e. $\boldsymbol{\beta}_X$, it is noted that Equ. (5) takes the usual form for the definition of parameter sensitivity. A graphical representation of the notion of sensitivity due to variations in the design parameters $\boldsymbol{\beta}_X$ and $\boldsymbol{\beta}_Y$ are shown in Figures 6(a,b), respectively. In Fig. 6(b), the tensor $\boldsymbol{L}_o \equiv \nabla_X \overset{\circ}{\bar{\boldsymbol{X}}}(\boldsymbol{Y}, t_o; \boldsymbol{\beta}_Y, \Delta\boldsymbol{\beta}_Y) = \overset{\circ}{\boldsymbol{F}}_Y \; \boldsymbol{F}_Y^{-1}$ refers to the design-velocity gradient. In the particular case of variations of the design parameter $\boldsymbol{\beta}_X$, the design velocity gradient is $\boldsymbol{L}_o = \boldsymbol{0}$ (Fig. 6(a)).

Design sensitivities with respect to variations in $\boldsymbol{\beta}_X$ are treated in an analogous fashion as in single stage parameter sensitivity analysis. We therefore consider here design sensitivity with respect to variations in the parameter $\boldsymbol{\beta}_Y$. Consider the dependence of $\tilde{\Phi}(\boldsymbol{X}, t)$ on $\boldsymbol{\beta}_Y$. This dependence results from the fact that the intermediate preform shape $\partial\boldsymbol{B}_o$ and the distribution Q (which represents a collection of variables e.g. $(\bar{\boldsymbol{F}}^p, s)$ that characterizes the intermediate preform $\boldsymbol{B}_o$) depend on $\boldsymbol{\beta}_Y$. In particular:

$$\tilde{\Phi}(\boldsymbol{X}, t; \boldsymbol{\beta}_Y) \;=\; \bar{\Phi}(\boldsymbol{Y}, t; \boldsymbol{\beta}_Y) = \; \bar{\Phi}(\boldsymbol{Y}, t; \partial\boldsymbol{B}_o(\boldsymbol{\beta}_Y), Q(\boldsymbol{\beta}_Y)) \tag{6}$$

Using equation (6) in equation (5), we can obtain that

$$\overset{\circ}{\Phi} = \frac{\partial \bar{\Phi}(\boldsymbol{Y}, t; \partial\boldsymbol{B}_o, Q)}{\partial(\partial\boldsymbol{B}_o)} \left[\frac{\partial(\partial\boldsymbol{B}_o)}{\partial\boldsymbol{\beta}_Y} [\Delta\boldsymbol{\beta}_Y] \right] + \sum_i \frac{\partial \bar{\Phi}(\boldsymbol{Y}, t; \partial\boldsymbol{B}_o, Q)}{\partial Q_i} \left[\frac{\partial Q_i}{\partial\boldsymbol{\beta}_Y} [\Delta\boldsymbol{\beta}_Y] \right] \tag{7}$$

To evaluate $\overset{\circ}{\Phi}$, one must first compute the Gateaux differentials of $\partial\boldsymbol{B}_o$ and Q with respect to a perturbation $\Delta\boldsymbol{\beta}_Y$ in the design parameters of all previous forming stages. These Gateaux differentials, which define perturbations in the intermediate preform shape and state can be used to compute the Gateaux differential of Φ in the current forming stage. Thus, the computation of sensitivities for multi-stage processes must be performed in a sequential manner. The independent driving forces for the computation of sensitivities in the current forming stage are the design differentials of $\partial\boldsymbol{B}_o$ and Q. The recognition of the linear dependence of $\overset{\circ}{\Phi}$ on these design differentials (Equ. (7)) enables the efficient computation of design sensitivities of the current forming stage, e.g., by incorporating the specific distribution $\overset{\circ}{Q}$ in the initial conditions of the sensitivity problem in the current forming stage.

Let us define $\Lambda_p = (\partial \boldsymbol{B}, Q)_p$ which essentially characterizes the preform after the p^{th} processing stage where $p \in [1, .., M]$ and assume that $\boldsymbol{\beta}_q$ characterizes the design space of the q^{th} processing stage. It is clear that $\frac{\partial \Lambda_p}{\partial \boldsymbol{\beta}_q} = 0, \; \forall \; p \in [1, .., q-1]$. One can compute the sensitivity of the preforms for $p \geq q$ by linear sensitivity relationships which take the form

$$\begin{bmatrix} \times & 0 & 0 & .. & 0 \\ \times & \times & 0 & .. & 0 \\ 0 & \times & \times & .. & 0 \\ .. & .. & .. & .. & .. \\ 0 & .. & \times & \times & 0 \\ 0 & .. & 0 & \times & \times \end{bmatrix} \begin{Bmatrix} \frac{\partial \Lambda_q}{\partial \boldsymbol{\beta}_q} \\ \frac{\partial \Lambda_{q+1}}{\partial \boldsymbol{\beta}_q} \\ .. \\ .. \\ \frac{\partial \Lambda_{M-1}}{\partial \boldsymbol{\beta}_q} \\ \frac{\partial \Lambda_M}{\partial \boldsymbol{\beta}_q} \end{Bmatrix} = \begin{Bmatrix} \times \\ \times \\ \times \\ .. \\ \times \\ \times \end{Bmatrix}$$

The above procedure is valid $\forall \; q \in [1, .., M]$ and for the purpose of optimization, gradients of the objective function and design constraints in a multi-stage process can be computed based on the knowledge of the design derivatives $\frac{\partial \Lambda_p}{\partial \boldsymbol{\beta}_q}$.

Let us now consider the mechanics in-between two forming stages. This phase usually consists of an unloading process where one of the dies is removed from contact with the workpiece. The unloading process is elastic and as a result there is no evolution of the intermediate relaxed (unstressed) configuration and the isotropic scalar internal variable s. The unloading process will therefore be modeled as a non-linear (finite deformation) elasto-static boundary value problem. If $\boldsymbol{B}$ represents the final configuration of the workpiece at the end of the loading phase with the total deformation gradient given as $\boldsymbol{F} = \boldsymbol{F}_X \boldsymbol{F}_Y = \boldsymbol{F}^e \; \bar{\boldsymbol{F}}^p$, then the solution to the unloading process results in the final body configuration $\boldsymbol{B}_u$ with the total deformation gradient given as $\boldsymbol{F}_u = \boldsymbol{F}^e_u \; \bar{\boldsymbol{F}}^p$. The workpiece material also undergoes a recovery process, whereby the material state evolves in the absence of an applied stress. The duration in-between forming stages is therefore characterized by the evolution of the inelastic internal variable s. The sensitivity deformation problem proposed here can also be used in the analysis of the sensitivity of the unloading process at the end of the forming stage. In this case, we need to consider the sensitivity of a finite deformation elasto-static problem. Thus, the sensitivity constitutive problem discussed above should be modified with the material deformation behavior treated as elastic in the unloading phase. The duration in between forming stages is characterized by the evolution of the sensitivity of the inelastic internal variable (recovery phase).

We note that within each forming stage, one could either use a total Lagrangian (reference configuration is the intermediate preform configuration $\boldsymbol{B}_o$) or an updated Lagrangian (reference configuration is updated during the incremental analysis of the current forming stage) sensitivity formulation. In the presentation here, it was assumed a total Lagrangian sensitivity formulation was used in each of the forming stages. These results can easily be extended to the case where an updated Lagrangian sensitivity formulation is used in the analysis of the forming stages. Using an updated Lagrangian analysis has been shown to be very appropriate for sensitivity analysis of deformation processes that requires extensive remeshing and data transfer operations. In addition, the use of an updated Lagrangian sensitivity analysis provides a unified mathematical framework for both shape and parameter sensitivity analyses. These issues will be discussed in detail in forthcoming publications.

In parallel to the above developments for multi-stage analysis, a number of algorithmic developments for single-stage sensitivity analysis remain to be addressed. They include (i) development of consistent adaptive remeshing techniques for simultaneous direct & sensitivity analyses, (ii) development of consistent data transfer techniques after remeshing for both the sensitivity and direct analyses, (iii) development of regularized contact sensitivity algorithms for multi-body contact, (iv) extending assumed strain methods to sensitivity analysis and other. Preliminary algorithms for some of these problems can be found in [61] and more work in this direction is currently in progress.

The above developments provide a clear picture of the proposed general mathematical framework for multi-stage forming processes using a continuum sensitivity analysis.

3.2.2 A sensitivity formulation for non-isothermal forming processes

Hot forming has been used extensively in manufacturing as a means to increase control of the microstructure during processing. It is common in multi-stage forming for several intermediate stages to be hot forming or purely thermal stages. For brevity, we discuss only hot forming processes where in addition to die, preform and other process parameter selection, one needs to select the thermal history of the die. Purely thermal processes are easier to handle and will not be discussed here.

A sensitivity analysis is being developed for large thermo-mechanically coupled hyperelastic-viscoplastic deformations. The discussion is limited to isotropic materials but further extensions are apparent. The proposed developments are consistent with our thermo-mechanical direct simulator discussed in [54].

In the constitutive sensitivity deformation sub-problem, linear sensitivity relationships which define the evolution of the hot plastic unstressed and the thermal configurations as a result of the perturbation in the design are developed (a decomposition $\boldsymbol{F} = \boldsymbol{F}^e\, \bar{\boldsymbol{F}}^p \boldsymbol{F}^\theta$ is assumed throughout this work). In particular, rate laws should be defined for the evolution of the state sensitivity field as well as for the evolution of the sensitivity of the plastic $\bar{\boldsymbol{F}}^p$ and thermal deformation gradients $\boldsymbol{F}^\theta$. Finally, the relationship between (a) $\overset{\circ}{\boldsymbol{T}}$ and $\overset{\circ}{\boldsymbol{F}}_{n+1}$ and (b) $\overset{\circ}{\boldsymbol{T}}$ and $\overset{\circ}{\theta}_{n+1}$ as required by the solution of the sensitivity thermo-mechanical problem need to be computed. As part of the update procedure, one computes the triad $\overset{\circ}{\boldsymbol{V}} = [\overset{\circ}{\boldsymbol{T}}, \overset{\circ}{\bar{\boldsymbol{F}}^p}, \overset{\circ}{s}]$ at the end of the time increment t_{n+1} where the sensitivity of the total deformation gradient $\overset{\circ}{\boldsymbol{F}}_{n+1}$ and the sensitivity of the temperature field $\overset{\circ}{\theta}_{n+1}$ are assumed known. The sensitivity $\overset{\circ}{\mathcal{W}}_{mech}$ of the mechanical dissipation $\mathcal{W}_{mech}$ is also computed as driving force for the thermal sensitivity problem at t_{n+1}. The mechanical dissipation is specified in terms of the plastic power by the empirical law $\mathcal{W}_{mech} = \ \omega\ \bar{\boldsymbol{T}} \bullet \bar{\boldsymbol{D}}^p = \ \omega\ \tilde{\sigma}\ \dot{\tilde{\epsilon}}^p$, where ω is the fraction of plastic power dissipated as heat.

Let us now consider the governing equations for the sensitivity deformation and thermal problems, respectively. We restrict our attention to parameter sensitivity problems and the extension of these ideas to shape sensitivity is straightforward. The weak form of the sensitivity deformation problem is given in section 2.1 and when concerned with thermo-mechanical deformations, the primary unknowns of Eq. (1) are the design differentials $\overset{\circ}{\boldsymbol{x}} = \hat{\overset{\circ}{\boldsymbol{x}}}(\boldsymbol{X}, t; \boldsymbol{\beta}, \Delta\boldsymbol{\beta})$ and $\overset{\circ}{\theta} = \hat{\overset{\circ}{\theta}}(\boldsymbol{X}, t; \boldsymbol{\beta}, \Delta\boldsymbol{\beta})$. The relationship between $\overset{\circ}{\boldsymbol{P}}$ and $[\ \overset{\circ}{\boldsymbol{x}}, \overset{\circ}{\theta}\ ]$ is obtained from the sensitivity constitutive problem.

Let us consider the sensitivity thermal equation by design differentiation of the energy equation:

$$\rho c \frac{\partial \overset{\circ}{\theta}}{\partial t} = \overset{\circ}{\mathcal{W}}_{mech} - \overset{\circ}{\overline{\nabla_x \bullet \boldsymbol{q}}} \tag{8}$$

where the constitutive equation for the heat flux $\boldsymbol{q}$ is given by Fourier's law with conductivity $K \geq 0$. Note that the sensitivity thermal problem is posed on the deformed configuration. After careful design differentiation followed by a temporal integration scheme (consistent with that used in the direct analysis), one obtains the weak-form of the time integrated thermal sensitivity equation posed on the deformed configuration $\boldsymbol{B} = \boldsymbol{B}_{n+1}$. Let ϑ represent an admissible sensitivity temperature field expressed over $\boldsymbol{B}$. Therefore a variational form of the thermal sensitivity equation is posed as:

$$\int_{\boldsymbol{B}} \frac{\rho c}{\Delta t}\left(\overset{\circ}{\theta}_{n+1} - \overset{\circ}{\theta}_n\right)\ \vartheta\ dV\ +\ \int_{\boldsymbol{B}} K \nabla_x\, \overset{\circ}{\theta}_{n+1} \bullet \nabla_x \vartheta\ dV\ +\ \int_{\partial \boldsymbol{B}} \left[\overset{\circ}{\boldsymbol{q}}_{n+1} + \boldsymbol{L}^T_{n+1}\boldsymbol{q}_{n+1}\right] \bullet \boldsymbol{n}\ \vartheta\ dA\ = \int_{\boldsymbol{B}} \overset{\circ}{\mathcal{W}}_{mech,n+1}\ \vartheta\ dV\ +\ \int_{\boldsymbol{B}} \left[\nabla_x \bullet (\boldsymbol{L}^T_{n+1}\boldsymbol{q}_{n+1}) + \nabla_x \boldsymbol{q}_{n+1} \bullet \boldsymbol{L}_{n+1}\right]\ \vartheta\ dV \tag{9}$$

where $\boldsymbol{L} = \overset{\circ}{\boldsymbol{F}}\ \boldsymbol{F}^{-1}$. The primary unknowns of Eq. (9) are $\overset{\circ}{\boldsymbol{x}} = \hat{\overset{\circ}{\boldsymbol{x}}}(\boldsymbol{X}, t; \boldsymbol{\beta}, \Delta\boldsymbol{\beta})$ and $\overset{\circ}{\theta} = \hat{\overset{\circ}{\theta}}(\boldsymbol{X}, t; \boldsymbol{\beta}, \Delta\boldsymbol{\beta})$. In order to obtain the final form of the variational sensitivity problem, the relationships between (a) $\overset{\circ}{\boldsymbol{F}}$ and $\overset{\circ}{\boldsymbol{x}}$ and (b) $\overset{\circ}{\mathcal{W}}_{mech}$ and $[\ \overset{\circ}{\boldsymbol{x}}, \overset{\circ}{\theta}]$ are needed. These relationships can be obtained as highlighted earlier.

The coupled discretized sensitivity deformation and thermal equations are linear and can be solved directly to yield the sensitivities $[\overset{\circ}{\boldsymbol{x}}, \overset{\circ}{\theta}]$ at time t_{n+1}. These developments enable the design of forming processes using thermal control. For example, the die thermal history can be tuned (e.g. via control of its surface heat flux/temperature) so that a final product is obtained with desired material properties.

Finally thermomechanical contact needs to be accounted for and this includes frictional heating, thermal softening at the interface properties, rate and state dependence of the frictional response and the effect of the mechanical properties on the heat transfer modes across the interface [66], [67]. A sensitivity formulation will be developed for thermo-mechanical contact that accounts for the above interfacial phenomena and accurately computes the sensitivities of the interface fields.

In summary, the thermo-mechanical sensitivity analysis highlighted here is novel, mathematically rigorous and capable of providing very accurate sensitivities. It can be easily incorporated within the multi-stage forming design simulator proposed in section 3.2.1.

3.2.3 Initial designs based on optimum deformation and microstructure evolution paths

In this section, we propose the calculation of optimum deformation paths/microstructure evolution paths that will be used as initial designs for the sensitivity based optimization algorithms presented earlier. Here, we restrict ourselves to minimum work paths (ideal paths) [68] but paths based on other criteria can be defined as well. Ideal forming methods have been mostly used in either steady-state or sheet forming [69]. Developments for non-steady state deformations of 'Tresca solids' are presented in [70].

Let us consider the following ideal forming problem: *Assume that the initial* $\boldsymbol{B}_i$ *and final configurations* $\boldsymbol{B}_f$ *of a workpiece in a given forming process are known. We want to find the deformation path that results in the least work.* In the remaining of this section, we will employ a model with an isotropic (scalar) state variable s. The problem of interest for a single material point (here $\tilde{\sigma}$ and $\dot{\tilde{\epsilon}}^p$ are the equivalent stress and strain-rate, respectively) is stated as follows:

$$\text{minimize} \quad w^p = \int_0^{t_f} \tilde{\sigma} f \; dt \;\; \text{subject to} \quad \dot{s} = g = h(s)\; f, \quad \text{where} \;\; f(\tilde{\sigma}, s) \;\equiv\; \dot{\tilde{\epsilon}}^p \tag{10}$$

The Euler-Lagrange equations for this minimization problem, can be shown to yield the following:[2]

$$\dot{\tilde{\sigma}} = -h \; f \; \frac{(2 f_s f_{\tilde{\sigma}} - f f_{\tilde{\sigma} s})}{(2 f_{\tilde{\sigma}}^2 - f f_{\tilde{\sigma}\tilde{\sigma}})} \tag{11}$$

The derivations here are more general than those in [8]–[9]. Based on the developments above, given a deformation gradient history, we can only check whether it constitutes an extremal path or not.

The extension of these ideas to non-homogeneous deformations can be done in two steps. Without loss of generality, the initial configuration $\boldsymbol{B}_i$ is discretized and material points $\mathbf{Y} \in \boldsymbol{B}_i$ are identified. The notation here refers to the multi-stage process of Fig. 5(a). The location of the material points $\tilde{\boldsymbol{x}}\,(\boldsymbol{Y}, t_f)$ in the final configuration $\boldsymbol{B}_f$ is assumed to be known, i.e. the deformation gradient $\boldsymbol{F}(t_f) = \nabla_Y \tilde{\boldsymbol{x}}\,(\boldsymbol{Y}, t_f)$ distribution is assumed. In the first step, we are simply looking for n intermediate stages. We make an initial guess of the deformation history by means of a spline approximation. The time domain is split into n equal parts and we know the value of the function $\tilde{\boldsymbol{x}}\,(\boldsymbol{Y}, t)$ at $t = 0$ and $t = t_f$. The intermediate n-1 values are initially guessed and a B-spline fitting is done. The gradient of this function with respect to $\boldsymbol{Y}$ gives the trial deformation gradient. If the process is a smooth deformation in a die, this amounts to guessing the equation of the die surface. Once an initial guess is formed, the constitutive problem is solved and the optimality condition is checked.

The assumed deformation gradient $\boldsymbol{F}(t_f)$ has been arbitrarily selected in the above procedure and hence a second step is needed to ensure uniqueness. In this step, the total work is expressed as:

$$W(\boldsymbol{x}_f) = \int_0^{t_f} \int_{\boldsymbol{B}_t} \bar{\boldsymbol{T}}' \cdot \bar{\boldsymbol{D}}^p dV_t dt \tag{12}$$

where the spatial location $\boldsymbol{x}_f = \tilde{\boldsymbol{x}}\,(\boldsymbol{Y}, t_f)$ is subject to the constraint that $\boldsymbol{x}_f \in \partial \boldsymbol{B}_f \;\; \forall\, \boldsymbol{Y} \in \partial \boldsymbol{B}_i$. The minimization of the total work W with respect to the unknown locations in the final configuration ensures the correct deformation gradient distribution $\boldsymbol{F}(t_f)$.

[2] For brevity, functional dependencies are dropped and subscripts are used to denote partial derivatives.

This approach does not enforce equilibrium at any intermediate time and only the kinematic and constitutive equations are satisfied with the material deforming on minimum work paths. The history of external forces can be computed as a post-processing step in order to enforce equilibrium at all intermediate times.

The algorithms above will be used to provide initial designs for preforms and dies. They are based however on work-minimization concepts and thus cannot be used to control the microstructure. A modification is proposed here to define optimum microstructure evolution paths. For example, let us assume that one is concerned with a single material point whose grain size $d(t)$ is evolving as (d can be thought of as one of the state variables s):

$$\dot{d} = \dot{d}(\dot{\bar{\epsilon}}^p, \theta, d) \tag{13}$$

Assuming that the desired grain size evolution is specified as $d^{\text{des}}(t)$, one can minimize the cost functional

$$E = \int_0^{t_f} (d(t) - d^{des}(t))^2 dt \tag{14}$$

A combination of minimum work/microstructure evolution paths will be examined. In addition, final state microstructure control problems will be implemented using such approaches.

Note that the temperature θ is an important variable in controlling the microstructure and the algorithms discussed above need to include θ. This enables the prediction of the heat flux history on the die surface that together with the material deformation can lead to a desired microstructure in the final product.

Once the ideal forming problem is solved, the intermediate configurations are known along with the necessary boundary tractions to maintain equilibrium. This information will be used intelligently in the choice of the various stages that correspond to this ideal deformation history while satisfying process constraints and account for any a-priori information (e.g. availability of tools, processes, etc.).

3.2.4 Multi-scale sensitivity fields and explicit microstructure optimization models

Let us assume that the behavior of the workpiece is described via a polycrystalline model referred to individual grains where attention is given to crystallographic texture [71]. Examples of FEM based modeling of texture are given in [72]-[76]. The desired texture in the final product is expressed in terms of three Euler angles $\{\phi_1, \Phi, \phi_2\}$, where classical Bunge notation is assumed. There is a one-to-one relationship between the Euler angles and the slip systems of a grain $(\boldsymbol{m}^\alpha, \boldsymbol{n}^\alpha)$. From an optimization point of view, it is useful to assume that the desired texture is given by its nodal values on a finite element grid that represents the microstructure at each point of the continuum and that interpolation of the Euler angles is applied within each element in that grid. In this sense, we can define the objective in the multi-stage process of Fig. 5(a) as follows (here $\boldsymbol{\beta}_Y$ represents the design parameters in the previous forming stages that are responsible for the microstructure of the preform shown in Fig. 5(a)):

$$I = \min_{\boldsymbol{\beta}} \sum_{j=1}^{M} \sum_{i=1}^{3} \|\phi_i(\boldsymbol{X}, t_{fin}; \boldsymbol{\beta}) - \phi_{i_{desired}}(\boldsymbol{x})\| \tag{15}$$

where $\phi_i = \{\phi_1, \Phi, \phi_2\}$ and M is the number of the sampling (Gauss integration) points in the continuum. The norm is referred to the domain defined by the N grains that constitute the underlying microstructure at each sampling point. Note that a significant number of variables define the complete microstructure distribution. Let Q represent the collection of $(\bar{\boldsymbol{F}}^p, s^\alpha)$ which characterizes the current state of all grains for all material points in the domain.

There are several mathematical issues to be addressed regarding the calculation of sensitivity fields based on polycrystalline constitutive models. For brevity, let us concentrate on the multi-stage process described in Fig. 5(a) and address the calculation of the sensitivity of the final texture at $t = t_f$ with respect to the initial material state and plastic deformation at $t = t_o$ in $\boldsymbol{B}_o$. This necessitates the solution of the sensitivity problem corresponding to a grain referred polycrystalline model posed as follows:

- Given $\boldsymbol{m}^{\alpha}_{n+1}$, $\boldsymbol{n}^{\alpha}_{n+1}$, $\boldsymbol{F}_{n+1}$, the triad $V_{n+1} = (\boldsymbol{T}_{n+1}, \bar{\boldsymbol{F}}^{p}_{n+1}, s^{\alpha}_{n+1})$ and $\overset{\circ}{Q}_n = (\overset{\circ}{\bar{\boldsymbol{F}}^{p}}_n, \overset{\circ}{s}{}^{\alpha}_n)$, calculate the linear relationship between the triad $\overset{\circ}{V}_{n+1} = (\overset{\circ}{\boldsymbol{T}}_{n+1}, \overset{\circ}{\bar{\boldsymbol{F}}^{p}}_{n+1}, \overset{\circ}{s}{}^{\alpha}_{n+1})$ and $\overset{\circ}{\boldsymbol{F}}_{n+1}$ for each grain at time t_{n+1} (incremental constitutive sensitivity problem)
- Solve the continuum sensitivity equilibrium equations with the averaged (of all the grains at a material point) sensitivity Cauchy stress (incremental kinematic sensitivity problem)

Note that the kinematic sensitivity problem above is essentially a macroscopic problem defined in terms of macro-length sensitivity fields (e.g. sensitivity of the average (over the grains at each integration point) Piola stress $\overset{\circ}{\boldsymbol{P}}$). The constitutive sensitivity problem is posed on a micro-length scale and relates the sensitivity of the microstructure (e.g. $\overset{\circ}{s}{}^{\alpha}_{n+1}$) to the macro-length sensitivities. Thus the two problems presented are coupled on 2 different length scales and can be solved to yield $\overset{\circ}{\boldsymbol{x}}$.

As a first step, one can introduce a number of a priori known textures and the assumptions that the texture at any point of the workpiece varies in a continuum fashion. Interpolation using the finite element discretization or even a global discretization in a more restricted parameter space can be sufficient for a number of microstructural design problems. Experimentation may be required for a particular type of processes (e.g. forging) to define a library of textures that someone can use in such an analysis. Note that documentation of experimentally observed textures in different forming processes is presented in [77]. Systematic documentation of textures in a given process obtained under varying process conditions has not yet been provided.

In addition to the above crystal plasticity models, a number of phenomenological models will be considered in our design analysis in particular for design of aircraft components made of multi-phase Ti-alloys [78]–[83]. In summary, we plan to develop multiple length scale sensitivity models to accommodate polycrystalline constitutive models and design of processes that lead to products with desired texture distribution.

3.2.5 Reliability analysis and robust process design

The deterministic design optimization of a metal forming process proves effective in systematically improving product quality and reducing manufacturing cost. Apart from discretization error, however, the modeling process itself could introduce considerable approximations in, for instance, the choice of constitutive law and the idealization of billet dimensions, material properties and die-workpiece contact conditions [84]. Therefore, it would be significant to estimate how the design criteria or constraints (e.g. geometric tolerances, microstructure and/or defects of final product) are influenced by such model uncertainties. This subsequently calls for a reliability-based design optimization (RBDO) [85, 86] such that the potential failure (rejection) probability [87] or reliability index [85] regarding to the design criteria or constraints is controlled to a prescribed economical level. For this purpose, additional derivatives of failure probability or reliable index function with respect to design variables need to be computed besides the previously proposed sensitivities [87].

3.2.6 Object oriented programming framework for the design of multi-stage forming processes

An important factor that has prevented research and development in the computational *design* of multi-stage processes is its complexity coupled with the fact that numerical simulations of forming processes have been programmed using traditional procedural languages. Our past experience with object oriented methods has shown that it is possible to develop reusable, efficient class structures for the analysis of single-stage forming processes that allows for the easy implementation, testing and maintenance of the simulator. In this project, we extend these ideas to the design of multi-stage processes.

A class `SingleStageProcessAnalysis` will be developed responsible for the direct and sensitivity analysis of thermo-mechanical processes like `Forging`, `Extrusion` etc. The functionality and data of the class `Direct` will be responsible for the direct analysis. The consistent (to the direct analysis) sensitivity analysis will be performed by the class `Sensitivity`. The derived class `CSM` will be introduced for the implementation of the CSM method discussed in this work. For multi-stage processes, development of the following class is proposed (left Box):

```
class MultiStageProcessAnalysis {
SingleStageProcessAnalysis current_stage;
SmartPointer <MultiStageProcessAnalysis>
                                   next_stage; }
```

```
class FormingSequence {
SmartPointer<MultiStageProcessAnalysis>
                                   first_stage;
Preform initial_product; }
```

The `SmartPointer<MultiStageProcessAnalysis>` points to the next stage (if any) of the process sequence. A feasible manufacturing process sequence is represented as shown (on the right) above. The initialization of these pointers is performed using knowledge based techniques and for this purpose the class `MultiStageProcessAnalysis` will also be provided with *intelligence* for reasoning for use in conjuction with knowledge based techniques. Thus different initializations lead to various feasible paths within which gradient based optimization analysis will be performed using the class `OptimizationAnalysis`. This class will obtain function and gradient information from the class `FormingSequence`. Commercial optimization software will be used to solve the majority of the required optimization problems.

4 PRELIMINARY DEFORMATION PROCESS DESIGN EXAMPLES

Two representative preliminary examples for metal forming design are presented here. The material chosen for the workpiece is 1100-Al at a temperature of 673 K [56]. The $\boldsymbol{F}$-bar method with a stabilization factor $\epsilon = 10^{-03}$ and four noded quadrilateral elements are used in the simulation [61]. A friction coefficient of 0.1 is assumed in the die-workpiece interface. Finally, Bézier curves are used for the representation of the dies and preforms with the control points of each curve used as design variables.

4.1 Two-Stage Forging Process of an Axisymmetric Disk

This example presents a forging process design for producing an axisymmetric ribbed disk. The initial billet is a cylinder of 2 mm in height and 0.8 mm in radius. A quarter of the billet is modelled in the simulation and design.

When a single stage process is applied, one can see that the die cavity cannot be fully filled in the upper-right corner as shown in Figure 7. In order to overcome this problem, a possible solution is the adoption of considerably more material than that required. However, this could lead to an unrealistically high forging force or to a sizeable increase in flash. An alternative solution to this problem is to apply a multi-stage process design, in which the initial billet (straight cylinder) is preformed to some intermediate shape using an open-die forging process. Then this preform is pressed to the desirable geometry with the given (closed-) finishing die. In the design process, the closed die keeps unchanged to form the desirable boundary of the final product. The objective here is to design the open die shape in the preforming stage such that the finishing die cavity can be completely filled:

$$\min_{\boldsymbol{\beta}} \; f(\boldsymbol{\beta}) \quad = \quad \frac{1}{N}\sum_{i=1}^{N} (x^i(\boldsymbol{\beta}) - x^{\text{desired}})^2 \tag{16}$$

where x^{desired} defines the desired boundary of the final product and N refers to the number of nodes on contact surface of the final product. To search for the optimum solution, the BFGS algorithm is employed.

A stroke of 0.6 mm and a ram speed of $V = 0.01$ mm/s are set for both the performing and finishing forging stages. The stoke is proceeded in 60 s using a time step of $\Delta t = 1.0\ s$ in the performing stage and $\Delta t = 0.5\ s$ in the finishing stage, respectively. During the design process, the volume of the workpiece remains unchanged.

Due to the large deformation of the workpiece during the forging processes, the finite element mesh is highly distorted particularly in the finishing stage. Therefore, remeshing operations must be applied. For the adopted remeshing criteria, remeshing was only performed in the finishing stage (Fig. 8) where an average of 16 remeshing operations was performed for each design iteration.

Figure 8 shows the design process of the performing die. The initial guess for the shape of the performing die is a straight line. From Figure 8 it can be seen that such a performing die does not lead to a finishing die cavity that is fully filled. As the optimization proceeds, the gap becomes smaller and smaller. After 7 design iterations, a perfect fill can be noticed from Figure 8. The convergence rate of the optimization process is clearly identified in Figure 9.

It is interesting to compare the forging forces between the non-optimized single stage process (using the initial billet directly forged with the finishing die, Fig. 7) with the optimized two-stage process, as shown in Figure 10. Obviously, the single stage process requires a higher force to accomplish the prescribed stroke, whereas the die cavity has not yet been fully filled. On the contrary, the force in the two-stage process is lower (by about 15 %) and the die is completely filled up.

4.2 Two-Stage Forging Process Design for Manufacturing of an Engine Disk

As an extension to the preceding example of axisymmetric ribbed disk forging, a practical problem with more complex geometry is described here, in which the final shape has two humps of equal height. The material and billet size are taken to be the same as in the earlier example. The full fill of the finishing die cavity is again adopted as the design objective.

A ram speed of $V = 0.01$ mm/s is assumed for both forging stages. The strokes of 0.7 mm and 0.5 mm are set for the performing and finishing stages, respectively. The stoke proceeds in 70 s using a time step of $\Delta t = 1.0$ s in the performing stage and then continues in 50 s with a step of $\Delta t = 0.4$ s in the finishing stage. As in the previous example, the volume of the workpiece remains unchanged during the design process. On average, one remesh operation is carried out in the preforming stage and 11 in the finishing stage, respectively, for each design iteration.

Figure 11 shows the design process of the performing die. When an initial guess of a straight line is given, a noticeable gap appears in the top of the outer cavity. After about 4 iterations, the die cavity has been practically fully filled. The convergence rate of the design process is shown in Figure 12.

5 Summary and Potential Impact of Proposed Work

As part of this DMII grant, we will extend our current activities in deformation process design to

- develop a general purpose continuum sensitivity analysis that can be used to design industrial multi-stage deformation processes
- allow control of the product properties and microstructure by proper process sequence selection and design of mechanical and thermal process parameters
- demonstrate the industrial relevance of the developed simulator with a variety of practical multi-stage forming design applications in aircraft manufacturing

The proposed simulator will enhance the design of industrial processes and result in an increased reliability and affordability. It will be used for the design of material, shape, and processing aspects of manufacturing for high performance metals leading to immediate economic benefits. Finally, this effort will solidify the transition from engineering analysis to engineering design in the area of materials processing currently driven by trial-and-error and knowledge-based techniques.

6 ACKNOWLEDGEMENTS

The work presented here is funded by the Engineering Design Division of DMII of the National Science Foundation (grant DMI-0113295). Additional support is provided by the Computational Mathematics program of the Air Force Office of Scientific Research (grant F49620-00-1-0373), by the Air Force Research Laboratory (grants TMC96-5835-0018-09-05 and TMC98–5835–0018-15) and by the Materials Process Design Group of the Alcoa Technical Center. The computing for this project was supported by the Cornell Theory Center. The principal investigator would also like to thank Dr. Srikanth Akkaram of General Electric Corporate Research and Development for his various technical contributions in the earlier stages of this work. Finally, the contributions of Dr. Qing Li and Shankar Ganapathysubramanian from our laboratory in preparing the preliminary examples given in this report are also acknowledged.

References

[1] Kobayashi S, Oh S and Altan T. Metal forming and the finite element method. 1989; *Oxford University Press* New York.

[2] Zhao G, Zhao Z, Wang T and Grandhi RV. Preform design of a generic turbine disk forging process. *J. of Materials Processing Technology* 1998; **84**: 193–201.

[3] Zhao G, Wright E and Grandhi RV. Forging reform design using the inverse die contact tracking method. *Num. Meth. Form. Proc.* (NUMIFORM'95). 1995: 643-648 (Balkema, Rotterdam).

[4] Biglari FR, O'Dowd NP and Fenner RT. Optimum design of forging dies using fuzzy logic in conjunction with the backward deformation method. *Int. J. Mach. T. Man.* 1998; **38**: 981-1000.

[5] Thomsen SG. Optimization of dies for axisymmetric cold forward extrusion. *Eng. Opt.* 1987; **11**: 13-20.

[6] Beckers M and Kopp R. A new approach to optimization of metal forming processes. *Numerical Methods in Industrial Forming Processes* 1989: 107-113 (Balkema, Rotterdam).

[7] Kusiak J. and Thompson EG. Optimization techniques for extrusion die shape design. *Num. Meth. Ind. Form. Proc.* 1989: 569-574 (Balkema, Rotterdam).

[8] Chung K and Richmond O. Ideal Forming - I: Homogeneous deformation with minimum plastic work. *Int. J. of Mechanical Sciences* 1992; **34(7)**: 575–591.

[9] Chung K and Richmond O. Ideal Forming - II: Sheet forming with optimum deformation. *Int. J. of Mechanical Sciences* 1992; **34(8)**: 617–633.

[10] Roy S, Ghosh S and Shivpuri R. Optimal design of process variables in multi-pass wire drawing by genetic algorithms. *J. of Manufacturing Science and engr.* 1996; **118**: 244–251.

[11] Chung JS and Hwang SM. Application of a genetic algorithm to the optimal design of the die shape in extrusion. *J. of Materials Processing Technology* 1998; **72**: 69–77.

[12] Chung JS and Hwang SM. Application of a genetic algorithm to process optimal design in non-isothermal metal forming. *J. of Materials Processing Technology* 1998; **80-81**: 136–143.

[13] Kim H, Altan T and Sevenler K. Computer aided part and processing sequence design in cold forging. *J. of Material Processing Technology* 1992; **33**: 57–74.

[14] Mehta BV, Ghulman H and Gerth R. Extrusion die design: A new methodology of using design of experiments as a precursor to neural networks. *J. of Metals (JOM)-e* 1999; **51(9)**.

[15] Vemuri, KR, Oh SI and Altan T. BID: A knowledge-based system to automate blocker design. *Int. J. Mach. T. Man.* 1989; **29**: 505-518.

[16] Coulter JP, Burke LI, and Demicri HH. Neural networks in materials processing and manufacturing: A review. *J. of Materials Processing and Manufacturing Science* 1993; **1**: 431–443.

[17] Kok S, Stander N and Roux W. Thermal optimization in transient thermoelasticity using response surface approximations. *Int. j. numer. meths. engr.* 1998; **43**: 1-21.

[18] Kok S and Stander N. Optimization of a sheet metal forming process using successive multipoint approximation. *Structural Optimization* 1999; **18**: 277-295.

[19] Tortorelli DA. Sensitivity analysis for non-linear constrained elastostatic systems. *Int. j. numer. meths. engr.* 1992; **33**: 1643-1660.

[20] Tortorelli DA and Michaleris P. Design Sensitivity Analysis: Overview and Review. *Inv. Prob. in Eng.* 1994; **1**: 71-105.

[21] Lee TH and Arora JS. Shape Design Sensitivity Analysis of Viscoplastic Structures. *Comp. Meth. Appl. Mech. Eng.* 1993; **108**: 237-259.

[22] Zabaras N and Yang G. A functional optimization and implementation for an inverse natural convection problem. *Comp. Meth. Appl. Mech. Eng.* 1997; **144**: 245–274.

[23] Tsay JJ and Arora JS. Nonlinear structural design sensitivity analysis for path dependent problems. Part 1: General theory. *Comp. Meth. Appl. Mech. Eng.* 1990; **81**: 183–208.

[24] Tsay JJ, Cardosa JEB and Arora JS. Nonlinear structural design sensitivity analysis for path dependent problems. Part 2: Analytical examples. *Comp. Meth. Appl. Mech. Eng.* 1990; **81**: 209–228.

[25] Badrinarayanan S and Zabaras N. A sensitivity analysis for the optimal design of metal forming processes. *Comp. Meth. Appl. Mech. Eng.* 1996; **129**: 319–348.

[26] Badrinarayanan S, Constantinescou A, Zabaras N. Preform design in metal forming. *Numerical meths. in Industrial Forming Processes*, Shen S-F, Dawson P (Eds) 1995; 533-538.

[27] Fourment L and Chenot JL. The Inverse Problem of Design in Forging. *Inverse Problems in Engineering Mechanics*, Bui HD et al. (Edts) 1994; 21-28 (Balkema, Rotterdam).

[28] Fourment L and Chenot JL. Optimal design for non-steady state metal forming processes - I. Shape optimization method. *Int. j. numer. meths. engr.* 1996; **39**: 33–50.

[29] Fourment L, Balan T and Chenot JL. Optimal design for non-steady state metal forming processes - II. Application of shape optimization in forging. *Int. j. numer. meths. engr.* 1996; **39**: 51–65.

[30] Noor AK, Needleman A and Peters JM. Sensitivity analysis for failure and damage in dynamically loaded tensile bars. *Comp. Meth. Appl. Mech. Eng.* 1998; **151**: 461–478.

[31] Kleiber M and Antúnez HJ, Hien TD, Kowalczyk P. Parameter sensitivity in non-linear mechanics - Theory and finite element computations. 1997; *John Wiley and Sons* New York.

[32] Antúnez HJ and Kleiber M. Sensitivity of forming processes to shape parameters. *Comp. Meth. Appl. Mech. Eng.* 1998; **137**: 189–206.

[33] Antúnez HJ. Thermo-mechanical modeling and sensitivity analysis for metal forming operations. *Comp. Meth. Appl. Mech. Eng.* 1998; **161**: 113–125.

[34] Vidal CA and Haber RB. Design sensitivity analysis for rate-independent elastoplasticity. *Comp. Meth. Appl. Mech. Eng.* 1993; **107**: 393–431.

[35] Kowalczyk P and Kleiber M. Shape sensitivity in elasto-plastic computations. *Comp. Meth. Appl. Mech. Eng.* 1999; **171**: 371–386.

[36] Mahnken R and Stein E. Parameter identification for finite deformation elasto-plasticity in principal directions. *Comp. Meth. Appl. Mech. Eng.* 1997; **147**: 17–39.

[37] Karaoglan L and Noor AK. Sensitivity analysis of frictional contact response of axisymmetric composite structures. *Computers and Structures* 1995; **55(6)**: 937–954.

[38] Antúnez HJ and Kleiber M. Sensitivity analysis of metal forming processes involving frictional contact in steady state. *J. of Materials Processing Technology* 1996; **60**: 485–491.

[39] Ghouali MA, Duvaut G, Ortola S, Oster A. Local analytical design sensitivity analysis of the forging problem using FEM. *Comp. Meth. Appl. Mech. Eng.* 1998; **163**: 55–70.

[40] Zhao G, Wright E and Grandhi RV. Preform die shape design in metal forming using an optimization method. *Int. j. numer. meths. engr.* 1997; **40**: 1213–1230.

[41] Joun MS and Hwang SM. Die shape optimal design in three dimensional shape metal extrusion by the finite element method. *Int. j. numer. meths. engr.* 1998; **41**: 311–335.

[42] Chung SH and Hwang SM. Optimal process design in non-isothermal non-steady metal forming by the finite element method. *Int. j. numer. meths. engr.* 1998; **42**: 1343–1390.

[43] Gao ZY and Grandhi RV. Sensitivity analysis and shape optimization for preform design in thermo-mechanical coupled analysis. *Int. j. numer. meths. engr.* 1999; **45**: 1349–1373.

[44] Byon SM and Hwang SM. Process optimal design in non-isothermal steady-state metal forming by the finite element method. *Int. j. numer. meths. engr.* 1999; **46**: 1075–1100.

[45] Doltsinis I and Rodic T. Process design and sensitivity analysis in metal forming. *Int. j. numer. meths. engr.* 1999; **45**: 661–692.

[46] Feng JP and Luo ZJ. A method for the optimal control of forging process variables using the finite element method and control theory. *J. Mat. Proc. Tech.* 2000; **108**: 40-44.

[47] Kim HS and Im YT. Multi-stage cold forging process design with a searching algorithm. *Transactions NAMRI/SME* 1996; **24**: 161-166.

[48] Malas JC et al. Optimization of Microstructure Development during Hot Working Using Control Theory. *Metallurgical and Materials Transactions A* 1997; **28A**: 1921-1930.

[49] Gao Z and Grandhi RV. Microstructure Optimization in Design of Forging Processes. *Int. J. of Machine Tools and Manufacture* 2000; 691-711.

[50] Lee SK, Ko DC and Kim BM. Optimal Die Profile Design for Uniform Microstructure in Hot Extruded Product. *Int. J. of Machine Tools and Manufacture* 2000; 1457-1478.

[51] Pietrzyk M, Glowacki M, Lenard JG. Numerical simulation of the evolution of the microstructure in closed-die forging. J. of Materials Processing Technology; 1994 **42**: 217-226.

[52] Devadas C, Samarasekara IV, and Hawbolt EB. The thermal and metallurgical state of steel strip during hot rolling: Part III. Microstructural evolution. *Metal. and Mater. Trans. A*; **22A**: 335-349.

[53] Domblesky JP and Shivpuri R. Grain size modeling and optimization of rotary forged Alloy 718. *J. of engr. Materials and Technology, Transactions of the ASME* 1997; **119**: 133-137.

[54] Zabaras N and Srikanth A. An OOP approach to the Lagrangian FEM analysis of large inelastic deformations and metal forming processes. *Int. j. numer. meths. engr.* 1999. **45(4)**: 399–445.

[55] Simo JC and Hughes TJR. Elastoplasticity and Viscoplasticity: Computational Aspects. 1998; *Springer-Verlag* Berlin.

[56] Brown SB, Kim KH and Anand L. An internal variable constitutive model for hot working of metals. *Int. J. Plast.*. 1989; **5**: 95-107.

[57] Kocks UF. Constitutive behavior based on crystal plasticity. 1987; 1-89 *Unified constitutive equations for creep and plasticity*, Miller AK (edt.) Elsevier.

[58] Bammann DJ. Modeling temperature and strain rate dependent large deformations of metals. *Appl. Mech. Rev.* 1990; **43 (5)**: 312-319.

[59] Zabaras N, Bao Y, et al. A continuum Lagrangian sensitivity analysis for metal forming processes with application to die design problems. *Int. j. numer. meths. engr.* 2000; **48**: 679–720.

[60] Srikanth A and Zabaras N. Preform design and shape optimization in metal forming. *Comp. Meth. Appl. Mech. Eng.* 2000; **190**: 1859–1901.

[61] Srikanth A, Zabaras N and Frazier WG. An updated Lagrangian finite element sensitivity analysis of large deformations using quadrilateral elements. *Int. j. numer. meths. engr.* 2000; **52**: 1131–1163.

[62] Srikanth A and Zabaras N. A gradient based optimization approach for the design of metal forming processes. 2000; **MED-11**: 495–507 *Advances in Metal Forming, Int. Mech. Eng. Congr. & Expos.*.

[63] Srikanth A. A continuum sensitivity analysis of large deformations with applications to metal forming design. 1990; *Ph. D. Thesis, Mechanical and Aerospace Engineering, Cornell University* New York.

[64] Nocedal J and Wright SJ. Numerical Optimization. 1999; *Springer Verlag* New York.

[65] Winstanley G. Artificial intelligence in engineering. 1991; *John Wiley and Sons* New York.

[66] Oancea VG and Laursen TA. A finite element formulation of thermomechanical rate-dependent frictional sliding. *Int. j. numer. meths. engr.* 1997; **40**: 4275–4311.

[67] Wriggers P and Miehe C. Contact constraints within a coupled thermomechanical analysis - A finite element model. *Comput. meths. Appl. Mech. Engrg.* 1994; **113**: (1994)

[68] Chung K and Richmond O. The mechanics of ideal forming. *J. Appl. Mech.* 1994; **61**: 176-181.

[69] Richmond O and Morrison HL. Streamlined wire drawing dies of minimum length. *J. of the Mechanics and Physics of Solids* 1967; **15**: 195-203.

[70] Richmond O and Alexandrov S. Nonsteady Planar Ideal Plastic Flow: General and Special Analytical Solutions. *J. Mech. Phys. Solids.* 2001; in press.

[71] Ortiz M. Computational micromechanics. *Compu. Mechanics* 1996; **18**: 1-18.

[72] Kalidindi SR, Bronkhorst CA and Anand L. Crystallographic texture evolution in bulk forming processing of FCC metals. *J. Mech. Phys. Solids* 1992; **40 (3)**: 537-569.

[73] Cuitino AM and Ortiz M. Computational Modeling of Single Crystals. *Modeling and Simulation in Mater. Sci. Engr..* 1992; **1**: 225-263.

[74] Marin EB and Dawson PR. On modeling the elastoplastic response of polycrystalline materials. *Comp. Meth. Appl. Mech. Eng.* 1998; **165**: 1-21.

[75] Marin EB and Dawson PR. Finite element analysis using an elasto-viscoplastic description of polycrystalline materials. *Comp. Meth. Appl. Mech. Eng.* 1998; **165**: 23-41.

[76] Beaudoin AJ, Mathur KK, Dawson PR and Johnson GC. Three-dimensional deformation process simulation with explicit use of polycrystal plasticity models. *Int. J. Plast.* 1993; **9**: 833-860.

[77] Kocks UF, Tome CN, Wenk HR, Beaudoin AJ. Tecture and Anisotropy. 2001; *Cambridge University Press.*

[78] Combres Y and Levaillant C. Modeling of the flow behaviour of a Ti6% Al - 4% V alloy at isothermal superplastic conditions. *Scripta Metallurgica.* 1990; **24**: 185-190.

[79] Combres Y and Levaillant C. Superplasticity of two-phased alloys: Qualitative and quantitative approach. *Int. J. Plasticity.* 1990; **6**: 505-519.

[80] Briottet I, Jonas JJ and Montheillet F. A mechanical interpretation of the activation energy of high temperature deformation in two phase materials. *Acta Metallurgica.* 1996; **44 (4)**: 1665-1672.

[81] Meier ML, Lesuer DR and Mukherjee AK. Alpha grain size and beta volume fraction aspects of the superplasticity of Ti6% Al - 4% V. *Materials Science and engr.* 1991; **A136**: 71-78.

[82] Yang HS, Gurewitz G and Mukherjee AK. Mechanical behaviour and microstructural evolution during superplastic deformation of Ti-6% Al - 4% V. *Mat. Trans. JIM* 1991; **32 (5)**: 465-472.

[83] Mosher D. A state variable material model for superplastic Titanium-6% Al-4% V. *Doctoral Thesis* Cornell University 1993.

[84] Sluzalec A, Simulation of stochastic metal-forming process for rigid-viscoplastic material, *Int. J. of Mechanical Sciences* 2000; **42**: 1935-1946.

[85] Wang L, Grandhi RV and Hopkins DA. Structural reliability optimization using an efficient safety index calculation procedure, *Int. j. numer. meths. engr.* 1995; **38**: 1721-1738.

[86] Tu J, Choi KK and Park YH., New study on reliability-based design optimization. *J. of Mechanical Design, Transactions of the ASME* 1999; **121**: 557-564.

[87] Santos JLT, Siemaszko A, Gollwitzer S and Rackwitz R. Continuum sensitivity method for reliability-based structural design and optimization. *Mech. Struct. Mach.* 1995; **23**: 497-520.

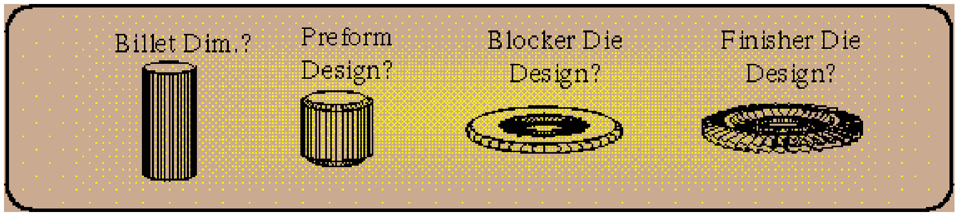

Figure 1: Typical sequence for a representative forming process (turbine engine disk forging).

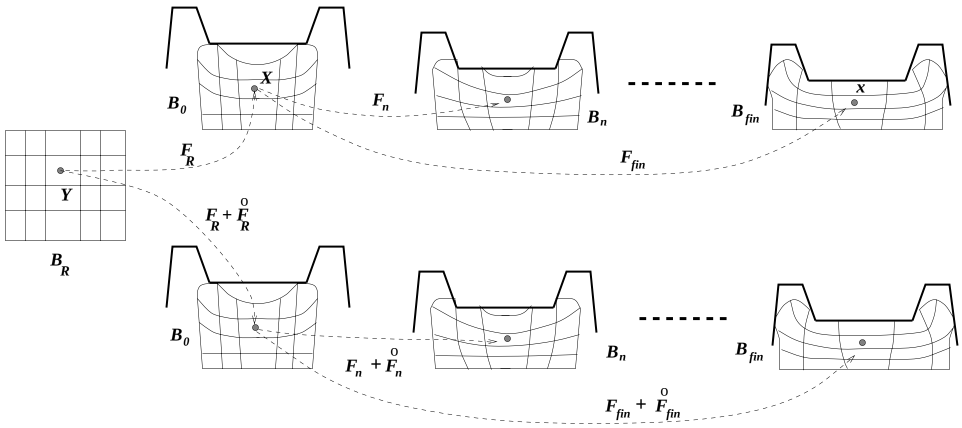

Figure 2: The shape derivative (i.e. the derivative with respect to the preform shape) $\overset{\circ}{\boldsymbol{F}}$ of the deformation gradient history. A closed die forging process is shown here for two (infinitesimally-close) preform shapes. The fixed configuration $\boldsymbol{B}_R$ is introduced to facilitate the definition of derivatives such as $\overset{\circ}{\boldsymbol{F}}$.

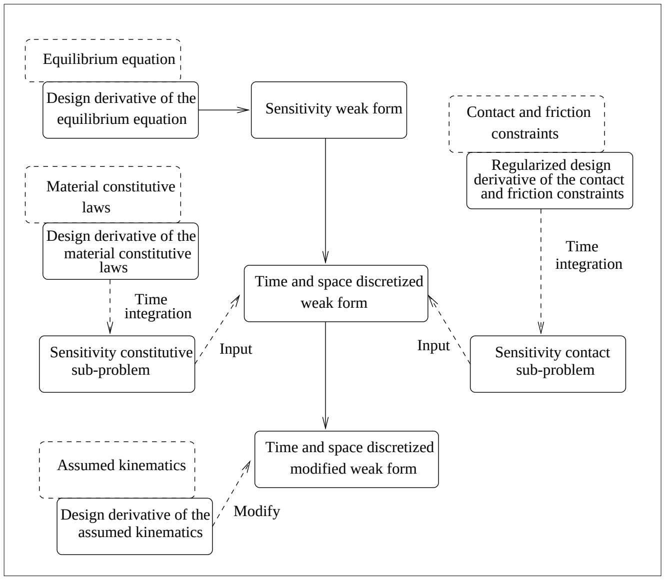

Figure 3: The continuum sensitivity algorithm. The three problems shown are linearly coupled and provide a single problem for computing the sensitivities of the deformation & material state: (a) constitutive problem determines the linear dependence of $\mathring{\boldsymbol{V}}_{n+1} = (\mathring{\boldsymbol{T}}_{n+1}, \mathring{\bar{\boldsymbol{F}}}^p{}_{n+1}, \mathring{s}_{n+1})$ on $\mathring{\boldsymbol{F}}_{n+1}$, (b) kinematic problem determines $\mathring{\boldsymbol{F}}_{n+1}$ knowing the linear relationship between $\mathring{\boldsymbol{V}}_{n+1}$ and $\mathring{\boldsymbol{F}}_{n+1}$, and by applying appropriate boundary conditions for $\mathring{\boldsymbol{F}}_{n+1}$, and (c) contact problem, where given the regions of contact and the subregions of sticking/sliding friction, one calculates the linear relation between the sensitivity $\mathring{\boldsymbol{\lambda}}$ of the contact traction and the sensitivity $\mathring{\boldsymbol{x}}$ of the deformation. s here denotes the state variables defining the microstructure evolution.

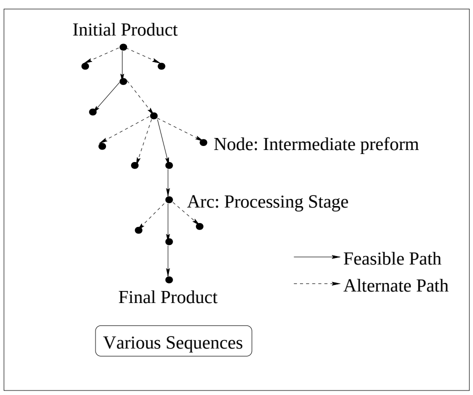

Figure 4: Schematic of a multi-stage forming sequence depicting various process sequences that can be used to convert the initial product to the final product. Each *directed arc* refers to a single stage process and is characterized by a design space which refers to the set of process parameters, dies used to deform the workpiece, annealing schedule etc. A directed arc (process) emanating from a given node is distinct (different) from all other arcs (from the same node) in the choice of the design space that characterizes it. Variations which can be resolved by appropriate choice of design parameters within the design space does not require a new arc.

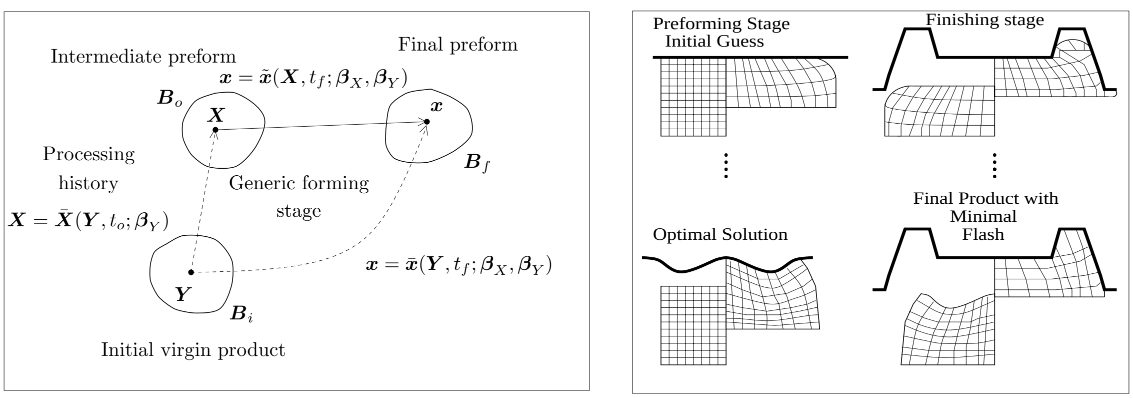

Figure 5: (a) Schematic of a generic forming stage. Note that the decomposition $\boldsymbol{F} = \boldsymbol{F}^e \bar{\boldsymbol{F}}^p \boldsymbol{F}^\theta$ is performed using the total deformation gradient $\boldsymbol{F} = \partial \boldsymbol{x} / \partial \boldsymbol{Y}$. (b) An example of a 2-stage design problem to clarify the concept of a 'previous forming stage' (here an open die forging process). The two stages are shown here during an iterative design process.

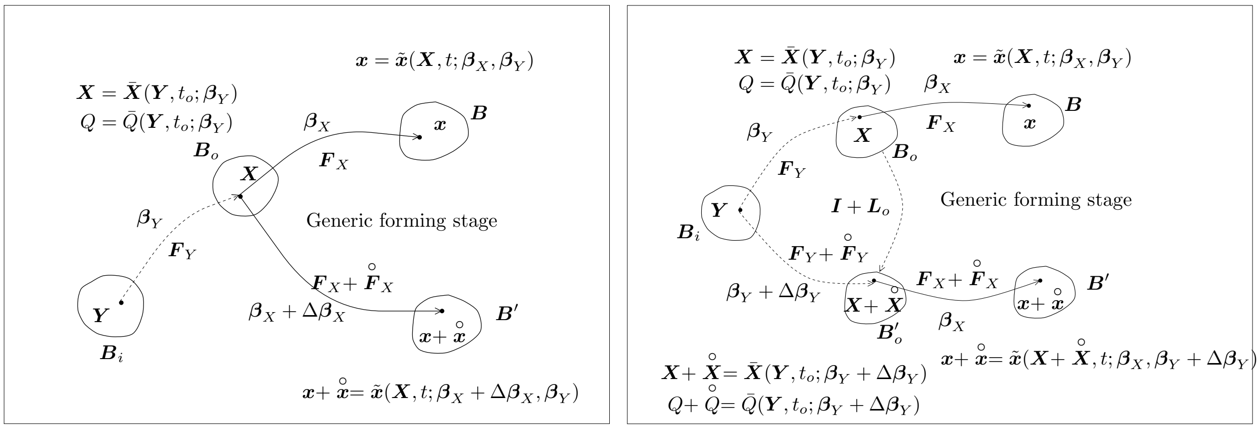

Figure 6: (a) Schematic representation of the design sensitivity of the deformation in the current forming stage due to variations in the (non-shape) design parameters of current forming stage. (b) Schematic representation of the design sensitivity of the deformation in the current forming stage due to variations in the design parameters of previous forming stages.

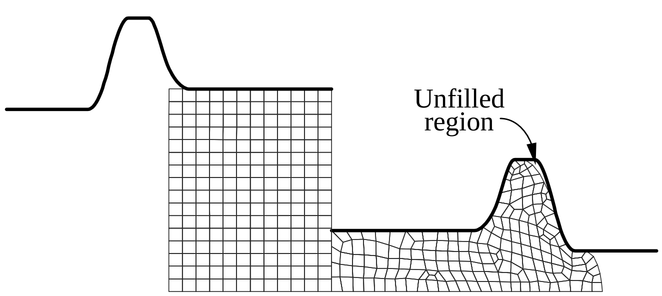

Figure 7: Single stage forging process for an axisymmetric ribbed disk (Example 1).

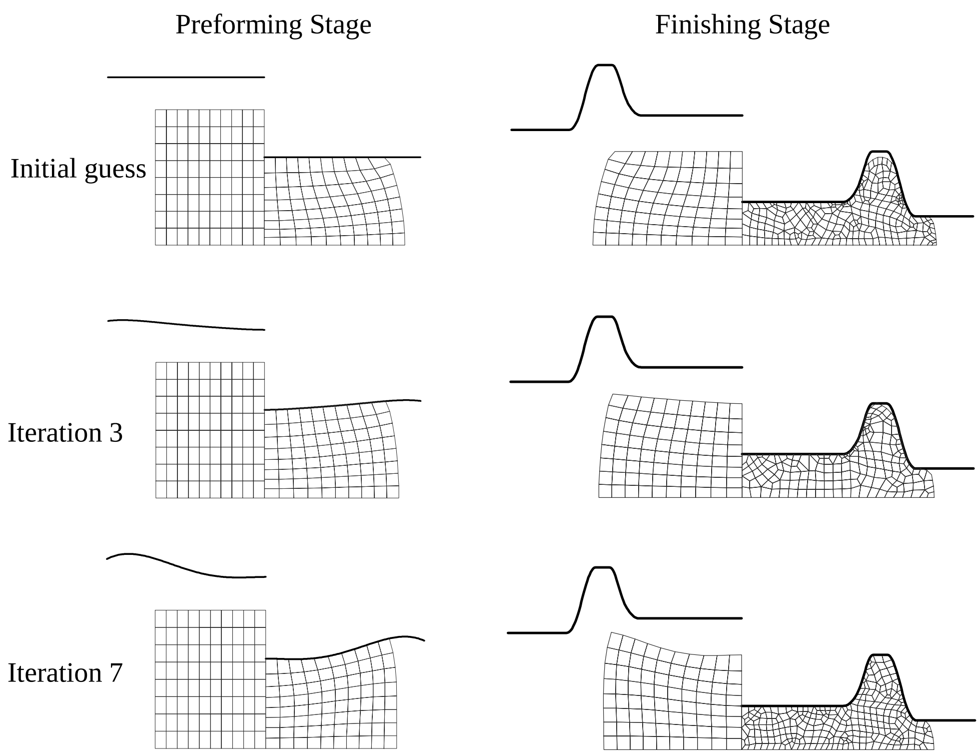

Figure 8: Two stage processes for an axisymmetric ribbed disk (Example 1).

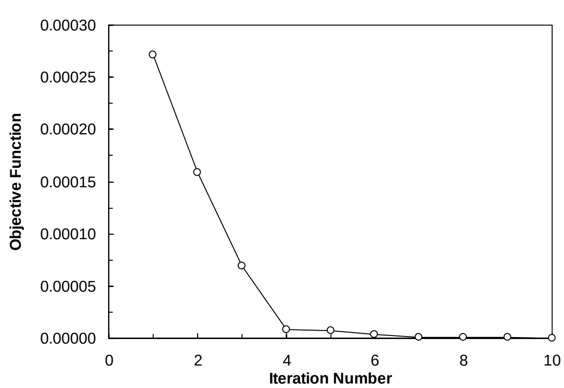

Figure 9: Convergence index of the optimization process (Example 1).

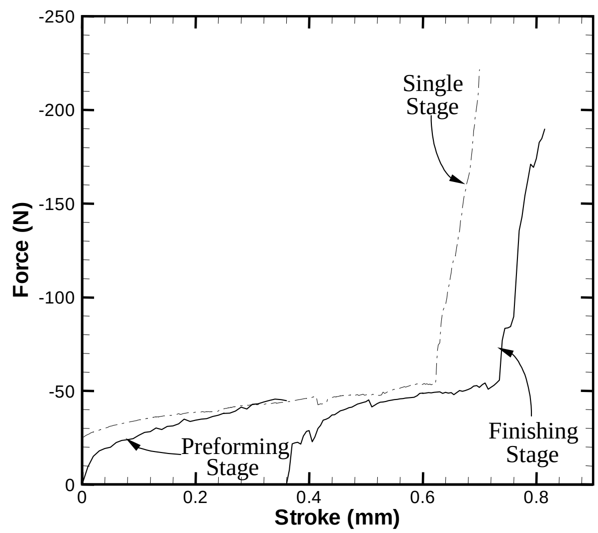

Figure 10: Comparison of the forces between the single-stage and two-stage designs (Example 1).

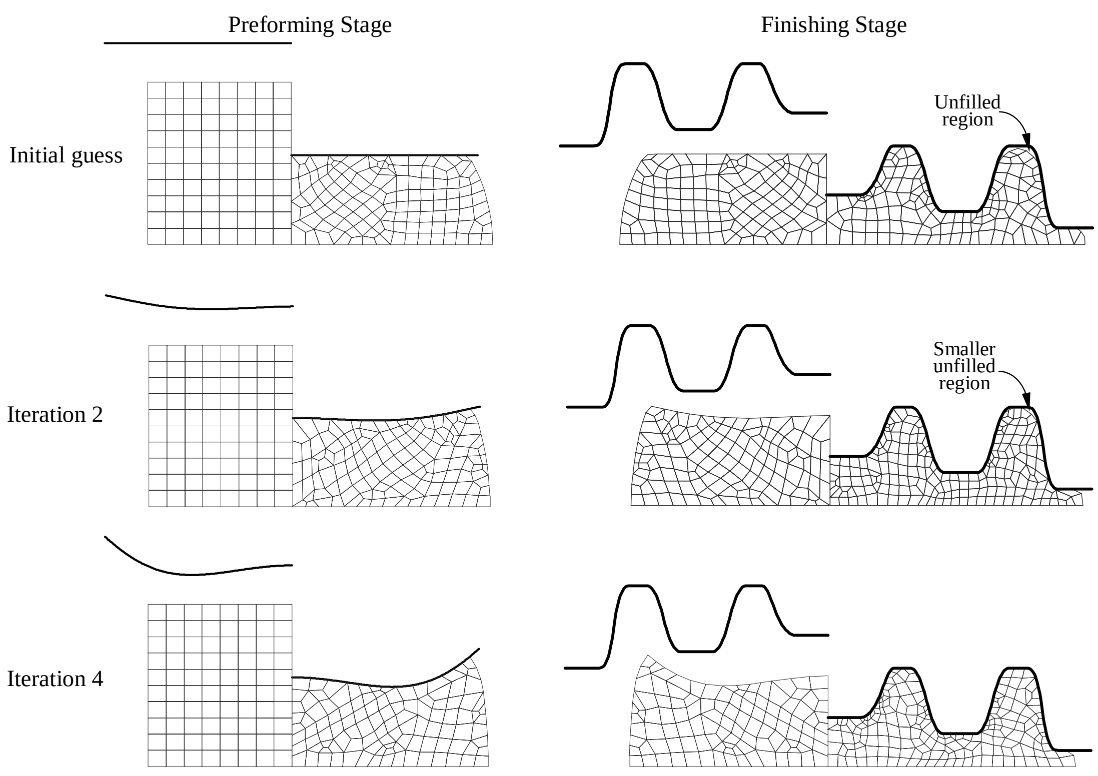

Figure 11: Shape optimization process of the preforming die for doubly-ribbed engine disk manufacturing (Example 2).

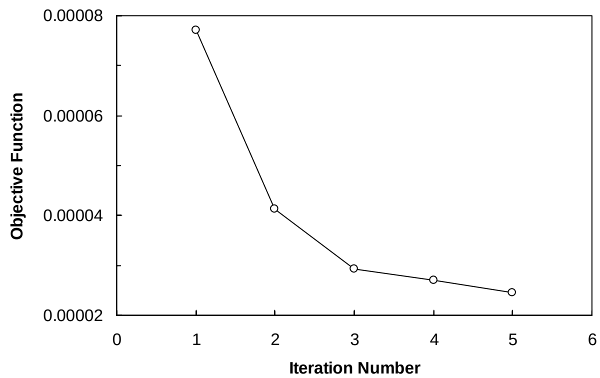

Figure 12: Convergence index for the design optimization problem (Example 2).